Archival Report

Schizophrenia Polygenic Risk During Typical Development Reflects Multiscale Cortical Organization

Matthias Kirschner, Casey Paquola, Budhachandra S. Khundrakpam, Uku Vainik, Neha Bhutani, Benazir Hodzic-Santor, Foivos Georgiadis, Noor B. Al-Sharif, Bratislav Misic, Boris C. Bernhardt, Alan C. Evans, and Alain Dagher

ABSTRACT

BACKGROUND: Schizophrenia is widely recognized as a neurodevelopmental disorder. Abnormal cortical development in otherwise typically developing children and adolescents may be revealed using polygenic risk scores for schizophrenia (PRS-SCZ).

METHODS: We assessed PRS-SCZ and cortical morphometry in typically developing children and adolescents (3–21 years, 46.8% female) using whole-genome genotyping and T1-weighted magnetic resonance imaging ($n = 390$) from the PING (Pediatric Imaging, Neurocognition, and Genetics) cohort. We contextualized the findings using 1) age-matched transcriptomics, 2) histologically defined cytoarchitectural types and functionally defined networks, and 3) case-control differences of schizophrenia and other major psychiatric disorders derived from meta-analytic data of 6 ENIGMA (Enhancing Neuro Imaging Genetics through Meta Analysis) working groups, including a total of 12,876 patients and 15,670 control participants.

RESULTS: Higher PRS-SCZ was associated with greater cortical thickness, which was most prominent in areas with heightened gene expression of dendrites and synapses. PRS-SCZ–related increases in vertexwise cortical thickness were mainly distributed in association cortical areas, particularly the ventral attention network, while relatively sparing koniocortical type cortex (i.e., primary sensory areas). The large-scale pattern of cortical thickness increases related to PRS-SCZ mirrored the pattern of cortical thinning in schizophrenia and mood-related psychiatric disorders derived from the ENIGMA consortium. Age group models illustrate a possible trajectory from PRS-SCZ–associated cortical thickness increases in early childhood toward thinning in late adolescence, with the latter resembling the adult brain phenotype of schizophrenia.

CONCLUSIONS: Collectively, combining imaging genetics with multiscale mapping, our work provides novel insight into how genetic risk for schizophrenia affects the cortex early in life.

https://doi.org/10.1016/j.bpsgos.2022.08.003

Schizophrenia is a multifaceted and heritable psychiatric disorder that is widely recognized to have a neurodevelopmental origin (1–3). Abnormal brain development likely predates the onset of clinical symptoms, which typically emerge in early adulthood (4). Genome-wide association studies (GWASs) support this hypothesis by showing that schizophrenia-related genes are involved in multiple neurodevelopmental processes (1,5). These genes may affect brain development, leading to vulnerability to environmental effects, and have been suggested to contribute to atypical cortical morphology, as previously observed in cohorts with a schizophrenia diagnosis (3).

Childhood and adolescent brain development involve dynamic and complex structural changes that are shaped by genetic and environmental factors (6–10). Longitudinal neuroimaging studies have consistently reported a global increase in cortical volume, thickness, and surface area that typically peaks in late childhood and is followed by decreases in

adolescence (7,10,11). At the same time, regional maturational trajectories are heterochronous, whereby sensory areas mature earlier than transmodal cortex (10,12,13), shaping large-scale patterns of cortical differentiation (14).

The neurodevelopmental hypothesis of schizophrenia posits that cortical maturation is perturbed, producing widespread cortical abnormalities (15). Differences in cortical morphometry are consistently reported across different stages and clinical phenotypes of the schizophrenia spectrum (16–18). However, investigating neurodevelopmental features of schizophrenia requires a departure from classic case-control designs. Alternatively, focusing on genetic risk enables us to investigate neuroanatomical correlates in a large population-based cohort of children and adolescents without interacting with disease-related factors (e.g., medication and chronicity). Recent work shows an effect of polygenic risk scores for schizophrenia (PRS-SCZ) on cortical morphometry (19–22),

though not necessarily gray matter volume (23–25). Thus far, studies have focused almost exclusively on adult cohorts. Only one study has investigated adolescents (aged 12–21 years) and noted an association of PRS-SCZ with globally decreased cortical thickness among cannabis users (19). Discerning neurodevelopmental aspects of genetic risk for schizophrenia requires investigation of younger cohorts.

Understanding the relation of genetic risk for schizophrenia to neurodevelopment can be further enhanced by contextualizing imaging-derived phenotypes of polygenic risk with maps of cortical organization. At the cellular level, a range of processes associated with healthy cortical development, such as synaptic pruning, dendritic arborization, and intracortical myelination, are implicated in the development of schizophrenia and may produce regional cortical disruptions (26–29). Recent advances in RNA sequencing (RNA-seq) of postmortem brain tissue (30) allow discernment of the relative contribution of cell types to patterns of atypical cortical morphometry (31,32). More complex interactions of microstructure and function on regional vulnerability may be captured by the groupings of cortical areas into cytoarchitectural types and functional networks. Indeed, recent studies of schizophrenia (17,33) and high PRS-SCZ in healthy adults (34) suggest differential sensitivity of histologically defined cytoarchitectural types (35) and functional networks (36). Finally, population-level effects of schizophrenia and other major psychiatric disorders can be used to illustrate the concordance of genetic risk for schizophrenia with disorder-related neuroanatomical phenotypes. Specifically, it can be tested how the association between genetic risk of schizophrenia and cortical morphometry in children and adolescents relates to shared and divergent neuroanatomical abnormalities across psychiatric disorders (32). Taken together, multiple scales of cortical organization can be used to provide a comprehensive description of the regional variations of an imaging-derived phenotype, such as genetic risk for schizophrenia.

Here, we address the relationship between PRS-SCZ and cortical organization in a large population-based cohort of typically developing children and adolescents (3–21 years) derived from the PING (Pediatric Imaging, Neurocognition and Genetics) study (37). We hypothesized that higher PRS-SCZ would be associated with atypical cortical morphometry (thickness, surface area, and volume). Then, we aimed to better understand the effect of PRS-SCZ on cortical morphometry by comparing the observed spatial patterns to cell type–specific gene expression, cytoarchitectural and functional differentiation, and cortical abnormalities seen in major psychiatric disorders. Finally, we examined age group–specific variations of high PRS-SCZ on cortical morphometry across different neurodevelopmental stages.

METHODS AND MATERIALS

Subjects

Neuroimaging, demographic, and genetic data of typically developing children and adolescents were derived from the PING study (37). The PING dataset is a wide-ranging, publicly shared data resource comprising cross-sectional data from 1493 healthy subjects. Participants were recruited and evaluated in the greater metropolitan areas of Baltimore, Boston,

Honolulu, Los Angeles, New Haven, New York, Sacramento, and San Diego using local postings and outreach activities. Written informed consent was given by parents for all PING subjects younger than 18 years. Participants between the ages of 7 and 17 years gave additional child assent, and all participants 18 years or older directly gave written informed consent. Exclusion criteria and more information about the PING cohort are described elsewhere (37). After quality control of genomic and imaging data (see below), a total of 390 participants from the PING dataset were included in this study. The mean age was 12.10 years (SD = 4.77, range = 3–21 years), and 46.8% were female (for more details, see Table S1).

Genomic Data

Genomic data processing and calculation of PRSs followed a recent publication from Khundrakpam *et al.* (38). Specifically, 550,000 single nucleotide polymorphisms were genotyped from saliva samples using the Illumina Human660W-Quad BeadChip (Illumina, Inc.). Details on imputation and preprocessing can be found in Supplemental Methods. After single nucleotide polymorphism imputation and preprocessing, 4,673,732 variants were available for calculation of PRSs. Participants were filtered to have at least 0.95 loadings to the European genetic ancestry factor (coded as "GAF_europe" in the PING dataset), resulting in 526 participants. To capture and quantify population structure, the same participants were used to calculate the 10 principal components across the variants, excluding areas in high linkage disequilibrium with each other (–indep-pairwise 50 5 0.2) with PLINK 2.

The PRS-SCZ was trained using results from the latest GWAS on schizophrenia at the time of analysis (39). The GWAS was filtered for having imputation quality over 90. Polygenic scores were calculated with PRSice 2.30e (40). Clumping of the data was performed using PRSice default settings (clumping distance = 250 kb, threshold r^2 = 0.1). To calculate the PRS-SCZ, we used the GWAS hits ($p < 5 \times 10^8$) cutoff criterion. This resulted in 86 variants common to the base and target datasets (Table S2). The choice of the GWAS hits threshold was made to increase the specificity of observed gene-brain associations for schizophrenia and to minimize the genetic overlap with other psychiatric disorders such as bipolar disorder (BD), which increases with lower PRS significance thresholds, including more single nucleotide polymorphisms. To illustrate this influence of PRS significance thresholds on the genetic overlap between schizophrenia and BD, we calculated PRS for BD by applying exactly the same processing pipeline (Supplemental Methods). In this sample, PRS-SCZ and PRS for BD did not correlate (r = 0.063) using the GWAS hits threshold chosen here, whereas applying lower significance thresholds, such as p = .05 and p = .1, resulted in moderate correlations (r = 0.254 and r = 0.286, respectively) (Figure S1).

Image Acquisition and Preprocessing

Details on image acquisition and preprocessing are described elsewhere (37). The CIVET processing pipeline (http://www.bic.mni.mcgill.ca/ServicesSoftware/CIVET, page 2.1) (41) was used to compute cortical thickness, surface area, and cortical volume measurements at 81,924 regions covering the entire

cortex, and quality control was performed by 2 independent reviewers (see Supplemental Methods for details). After quality control of the total 526 subjects who passed filtering for European genetic ancestry, a total sample size of 390 participants remained for all subsequent analyses.

Statistical Analyses

Association Between PRS-SCZ and Cortical Morphometry. To identify the association of PRS-SCZ with vertexwise cortical thickness, surface area, and cortical volume, general linear models were applied using the SurfStat toolbox (http://www.math.mcgill.ca/keith/surfstat/) (42). Each cortical feature was modeled as

$$
\begin{aligned}
T_i = \ & \text{intercept} + \beta_1\text{PRS-SCZ} + \beta_2\text{Age} + \beta_3\text{Age}^2 \\
& + \beta_4(\text{PRS-SCZ} * \text{Age}) + \beta_5(\text{PRS-SCZ} * \text{Age}^2) \\
& + \beta_6\text{Sex} + \beta_7\text{PC10} + \beta_8\text{Scanner} + \beta_9\text{BrainVolume} + \varepsilon_i
\end{aligned}
\tag{1}
$$

where i is a vertex, PRS-SCZ is the PRS for schizophrenia, Age is years at the time of scan, PC10 are the first 10 principal components of genomic data to account for population stratification, ε is the residual error, and the intercept and the β terms are the fixed effects. Models with quadratic age terms were chosen because they fit the data better than models with only lower degree age terms (Supplemental Methods). For

each cortical feature, vertexwise t statistics of the association with PRS-SCZ (β_1PRS-SCZ) were mapped onto a standard cortical surface. To assess the significance of PRS-SCZ effects on each of the 3 different cortical features, whole-brain correction for multiple comparisons using random field theory (RFT) at cluster-level $p \leq .01$ (43,44) was applied. Notably, only cortical thickness showed a significant association with PRS-SCZ after RFT correction (see Results, Figure 1); all subsequent analyses were thus restricted to cortical thickness only.

Cellular Composition of the Cortex and PRS-SCZ Effects on Cortical Thickness. We evaluated how the observed pattern of PRS-SCZ effects on cortical thickness relates to regional variations in the cellular compositions of the cortex. Given prior evidence (45) and histological validation (Supplemental Methods), we focused on components of the neuropil—namely glial cell processes, axons, dendritic trees, and neuron-to-neuron synapses—that are cortical tissues other than cell bodies or blood vessels. Neuropil-related gene expression was calculated by combining tissue-level RNA-seq (available online at http://development.psychencode.org/) (46) with gene lists of cell types, based on single-cell RNA-seq (30), and gene lists of neuron compartments, based on gene ontologies (47,48). Tissue-level RNA-seq provided expression levels of 60,155 genes in 11 neocortical areas (46). The areas were cytoarchitecturally defined in each specimen, supporting
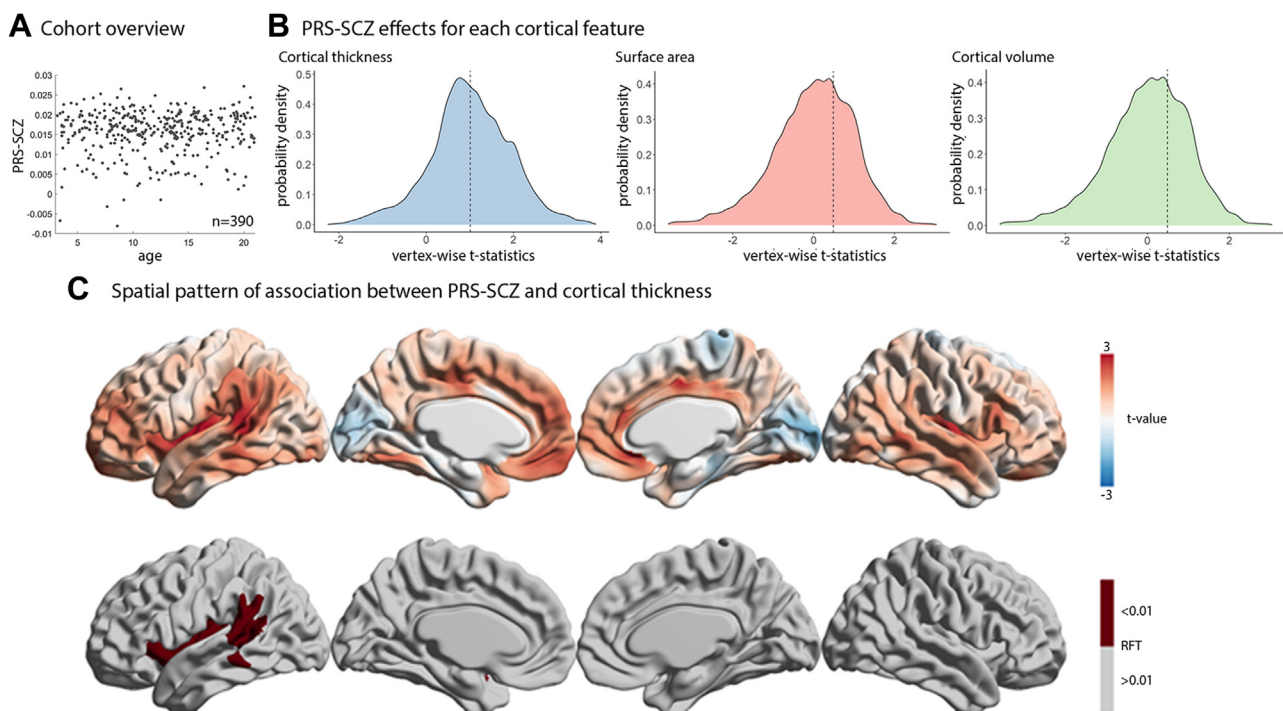

Figure 1. Association of polygenic risk scores for schizophrenia (PRS-SCZ) with cortical morphometry. **(A)** Scatterplot shows that PRS-SCZ varies across the age range, without being correlated with age. **(B)** Probability distributions show the variation in vertexwise t values of the association of PRS-SCZ with each cortical feature. Dashed lines represent the mean values of each cortical feature. Only cortical thickness was significantly shifted from 0. **(C)** Unthresholded (top) and thresholded (bottom) maps after random field theory (RFT) correction ($p < .01$) show the association of PRS-SCZ with cortical thickness. Unthresholded maps for surface area and cortical volume are Figures S2 and S3.

precise mapping and comparison across individuals. Crucially, we selected 12 brain specimens from the PsychEncode developmental dataset that were age-matched to the PING imaging cohort (3–21 years) because gene expression differs substantially between children and adults (49). Single-cell RNA-seq (30) provided specificity scores of each gene to glial cell types. For each type, we weighted the genes by the specificity score, then calculated the average across genes, across specimens, and within area. For each neuron compartment, we defined a list of marker genes using the Gene Ontology KnowledgeBase, then calculated the average expression of marker genes in each area and specimen. The annotated terms used were "neuron_to_neuron_synapse," "dendritic_tree," and "main_axon." Next, we mapped the 11 areas to the cortical surface and extracted area-average PRS-SCZ effects on cortical thickness. The cortical areas were visually matched to the nearest parcel in a 200-parcel decomposition of the Desikan-Killiany, as performed in previous work (50). Finally, we tested the spatial similarity of cell type–specific gene expression with PRS-SCZ effects on cortical thickness using product-moment correlations. Statistical significance was determined relative to random reassignment permutation tests (10,000 repetitions).

Aggregation of PRS-SCZ Effects on Cortical Thickness by Cytoarchitectural Type and Functional Network.

Given the hierarchical properties of cortical development (10) and given that disease-related imaging phenotypes are guided by different modes of cortical organization (17,33,51), we sought to contextualize the PRS-SCZ effects on cortical thickness by cytoarchitectural types and intrinsic functional networks. A whole-cortex atlas of cytoarchitectural types was acquired (https://github.com/caseypaquola/DMN) (52), which reflects an intersection of the classic Von Economo atlas of cortical areas (53,54) with a recent re-analysis of Von Economo micrographs that categorized the areas according to type (35). Cortical types synopsize degree of granularity, from high laminar elaboration in koniocortical areas, 6 identifiable layers in eulaminate III-I, poorly differentiated layers in dysgranular, and absent layers in agranular.

Functional networks were defined based on the Yeo atlas (https://github.com/ThomasYeoLab/CBIG) (36). The atlas reflects clustering of cortical vertices according to similarity in resting-state functional connectivity profiles acquired in 1000 healthy young adults. We assessed whether the PRS-SCZ effects on cortical thickness were stronger or weaker within each cortical class or functional network relative to spin permutations that preserve spatial autocorrelation (55,56) (see Supplemental Methods for details).

Pattern Similarity Between PRS-SCZ Effects and Cortical Abnormalities in Major Psychiatric Disorders.

We assessed whether cortical thickness differences of PRS-SCZ relate to patterns of cortical thickness abnormalities observed in major psychiatric disorders including schizophrenia, BD, major depressive disorder (MDD), attention-deficit/hyperactivity disorder (ADHD), autism spectrum disorder, and obsessive-compulsive disorder. To this end, the PRS-SCZ–related t-statistic map was parcellated into 64 Desikan-Killiany atlas regions (57) and then correlated with the corresponding Cohen's d maps derived from recently published meta-analyses by the ENIGMA schizophrenia (15), BD (58), MDD (59), ADHD (60), obsessive-compulsive disorder (61), and autism spectrum disorder (62) working groups, as implemented in the ENIGMA toolbox (63). Specifically, spatial pattern similarity of cortical Desikan-Killiany maps was examined using product-moment correlations. Statistical significance accounting for spatial autocorrelation was assessed with the spin permutation tests (10,000 repetitions) (55,56) implemented in the ENIGMA toolbox (63). The medial wall was assigned as a NaN and not included in any permuted correlation (64). Statistical significance was deemed where $p_{spin} <$ .025 (two-tailed test), and false discovery rate ($p_{FDR} <$ .05) was applied to control for multiple comparisons ($n = 6$).

Age Group Effects of PRS-SCZ on Cortical Thickness.

We examined the distinctiveness of PRS-SCZ–related cortical thickness differences in different neurodevelopmental stages by dividing the sample into 3 age groups; early childhood (3–9 years, $n = 145$), early adolescence (10–15 years, $n = 155$), and late adolescence (16–21 years, $n = 116$) (65). The PRS-SCZ effect on cortical thickness was evaluated within each group using the above-mentioned general linear models (equation 1). However, the age term was centered to the mean of the group to focus on the effect within the specified developmental stage (8). Note that there was no correlation between age and PRS-SCZ scores ($r = 0.058$) (Figure 1A). We specifically examined whether the association of the PRS-SCZ effect with the adult cortical thickness phenotype of SCZ changed across age groups. To do so, we compared the product-moment correlation coefficients between age group and whole cohort t-statistic maps (66).

RESULTS

Polygenic Risk for SCZ Is Associated With Greater Cortical Thickness

To test the association between PRS-SCZ and cortical morphometry in typically developing children and adolescents, we used T1-weighted MRI and whole-genome genotyping ($n = 390$) from the PING cohort (3–21 years, mean ± SD = 12.1 ± 4.7 years, 46% female) (Table S2). Vertexwise general linear models related cortical thickness with PRS-SCZ, controlling for age, sex, the first 10 principal components of genetic variants (to account for population stratification), scanner, and total brain volume. We found that higher PRS-SCZ was significantly associated with greater cortical thickness (RFT corrected, $p <$ .01) but not surface area or cortical volume (Figure 1B; Figures S2 and S3). Overall, the unthresholded t-statistic map revealed that higher PRS-SCZ was associated with widespread increases in cortical thickness in association cortex but reduced cortical thickness in sensory areas (Figure 1C, top). Higher PRS-SCZ was associated with significantly thicker cortex in the left insula, left superior temporal gyrus, and left inferior parietal lobule (Figure 1C, bottom) (RFT corrected, $p <$ .01). These results suggest a significant

effect of PRS-SCZ on cortical thickness but not surface area or cortical volume in typically developing children and adolescents. As such, subsequent analyses are restricted to cortical thickness.

In the next step, we sought to examine how the PRS-SCZ–related cortical thickness increase in typically developing children and adolescents relates to different levels of cortical organization, including 1) cell type–specific gene expression, 2) cytoarchitectural and functional systems, and 3) cortical pattern of case-control differences from schizophrenia and other major psychiatric disorders.

Alignment With Cell Type–Specific Gene Expression

Histological examinations have reported a null or minimal relationship between cortical thickness and neuron number in healthy brain samples (67–69). Instead, regional variations in cortical thickness show a strong association with neuropil (69), the portion of cortical tissue that excludes cell bodies or blood vessels (70). We examined whether cortical thickness differences related to PRS-SCZ mirrored regional variations in the neuropil composition of the cortex to generate hypotheses on the neuropil components affected by PRS-SCZ. To this end, we first validated the relation between cortical thickness and neuropil using tabular data and photomicrographs of Nissl stains ($r = 0.49$, $p_{spin} = .018$) (Figure 2A) (53,71). In contrast, neuronal density was not correlated with histologically defined cortical thickness ($r = 0.08$, $p_{spin} = .678$), which aligns with the findings of previous work (68,69). Then, we estimated regional variations in neuropil-related gene expression based on 6 cellular components (astrocytes, microglia, oligodendrocytes, axons, dendritic trees, and neuron-to-neuron synapses) by combining tissue-level RNA-seq (46) with single-cell RNA-seq for cell types (30) and gene ontologies for neuron compartments (47,48) (Figure 2B). Correlating PRS-SCZ effects on cortical thickness with neuropil-related gene expression, we found that PRS-SCZ effects are significantly associated with gene expression for dendritic trees ($r = 0.755$, $p_{perm} = .006$), synapses ($r = 0.618$, $p_{perm} = .005$), and at a trend level with axons ($r = 0.481$, $p_{perm} = .069$) (Figure 2C). In contrast, no significant correlation was observed with gene expression related to glial components of neuropil (Figure 2C). Together, these analyses suggest that greater cortical thickness with higher PRS-SCZ is observed in areas with greater dendritic and synaptic density.

Contextualization by Cytoarchitectural Types and Functional Networks

Next, we aimed to determine whether the PRS-SCZ is preferentially associated with certain cytoarchitectural types or functional networks. Based on established atlases of cytoarchitectural and functional differentiation (35,36), we found that the PRS-SCZ effect was stronger than null models in the ventral attention network (median $\pm$ SD = 1.64 $\pm$ 0.88, $p_{spin} = .004$). Conversely, the PRS-SCZ effect was weaker or more negative than null models in the koniocortical type (i.e., primary sensory areas) (median $\pm$ SD = 0.08 $\pm$ 1.10, $p_{spin} = .008$) (Figure 3).

Thickness Signatures of PRS-SCZ and Major Psychiatric Disorders

We assessed whether PRS-SCZ effects on cortical thickness relate to abnormal cortical thickness patterns observed in case-control meta-analyses (Cohen's d maps) of schizophrenia and other psychiatric illnesses. The PRS-SCZ–related cortical thickness increase showed a negative correlation with schizophrenia-related cortical abnormalities ($r = -0.326$, $p_{spin} = .0022$). In addition, we found similar negative correlations to cortical abnormalities in BD ($r = -0.466$, $p_{spin} < .001$), MDD ($r = -0.538$, $p_{spin} < .001$), and ADHD ($r = -0.430$, $p_{spin} < .001$) but not obsessive-compulsive disorder or autism spectrum disorder (Figure 4). To further test whether the correlation between PRS-SCZ–related cortical thickness differences and schizophrenia-related cortical thinning was significantly different compared with the correlations observed in non-SCZ psychopathologies, we applied pairwise comparisons of the correlation coefficients of schizophrenia with those from BD, MDD, and ADHD using the R package cocor (72) and the confidence interval test from Zou (73). The confidence intervals for each comparison of correlations r included zero (correlation r: SCZ vs. BD, 95% CI, −0.01 to 0.30; SCZ vs. MDD, 95% CI, −0.03 to 0.45; SCZ vs. ADHD, 95% CI, −0.20 to 0.39). This shows that the correlation of PRS-SCZ cortical thickness differences with the schizophrenia-related cortical thickness abnormalities was not significantly different compared with the correlations with each of the other major psychiatric disorders. Altogether, cortical regions showing PRS-SCZ–related greater thickness are those with the strongest thinning across disease maps of schizophrenia and
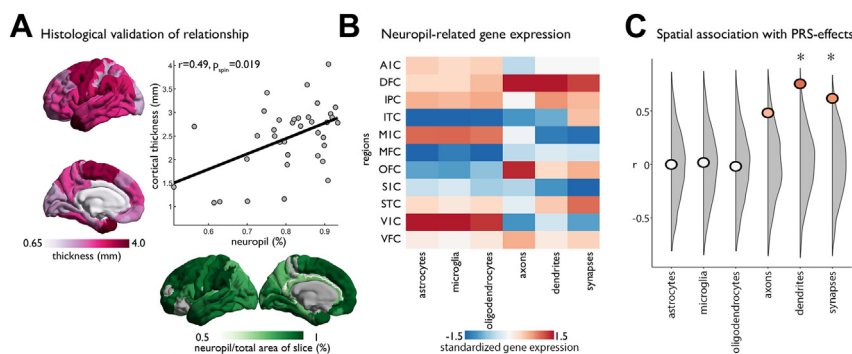

Figure 2. Decoding spatial patterns of polygenic risk scores for schizophrenia (PRS-SCZ) on cortical thickness. **(A)** Correlation of histological measurements of cortical thickness and neuropil from Von Economo and Koskinas (53). Cortical thickness is shown in pink and on the y-axis. Neuropil is shown in green and on the x-axis. **(B)** Gene expression varies across glial and neuron-related compartments of neuropil in 11 cortical regions. **(C)** Correlation of neuropil-related gene expression with the PRS-SCZ effects showed significant association with dendrites and synapses, compared with null distributions from permutation testing (gray). A1C, primary auditory cortex; DFC, dorsal frontal cortex; IPC, inferior parietal cortex; ITC, inferior temporal cortex; M1C, primary motor cortex; MFC, medial frontal cortex; OFC, orbital frontal cortex; S1C, primary somatosensory cortex; STC, superior temporal cortex; V1C, primary visual cortex; VFC, ventral frontal cortex.

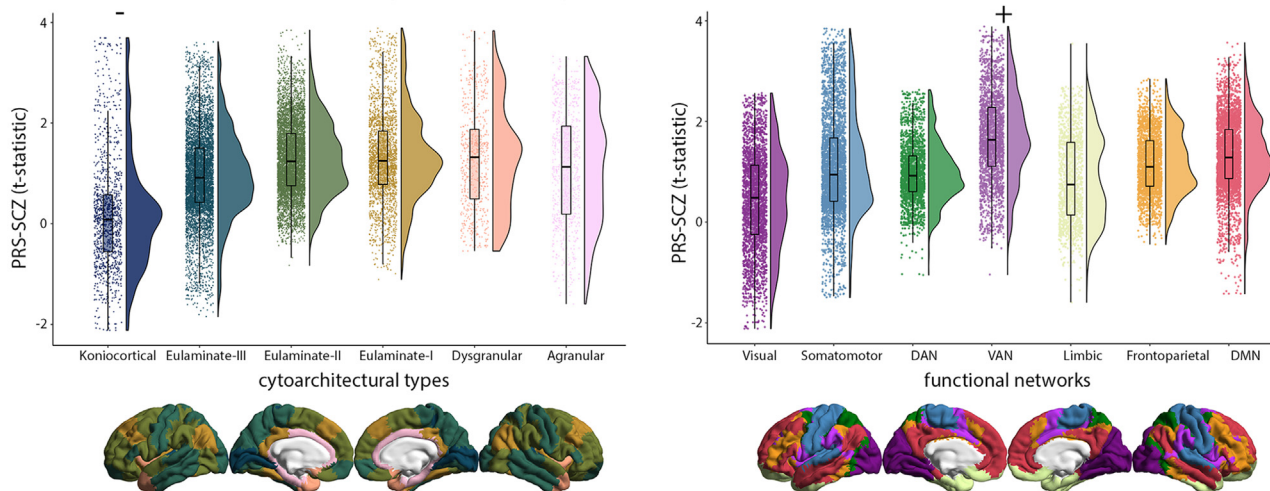Aggregation of PRS-SCZ effect within cytoarchitectural types and functional networks

Figure 3. Aggregation of the polygenic risk scores for schizophrenia (PRS-SCZ) effect within cytoarchitectural types and functional networks. Raincloud plots show the distribution of the PRS-SCZ effect on cortical thickness stratified by cytoarchitectural type (35) and functional network (36). Relative to spin permutation null models, the koniocortical cortical type encompassed significantly lower *t* statistics, whereas the ventral attention network (VAN) encompassed significantly higher *t* statistics. DAN, dorsal attention network; DMN, default mode network.

genetically related affective disorders (e.g., BD, MDD, and ADHD).

Age Group Effects of PRS-SCZ

Schizophrenia-related genes are implicated in neuro-developmental processes, and as such, the effect of PRS-SCZ on cortical thickness likely varies with age. Although the cross-sectional nature of this cohort prohibits mapping the individual trajectories of cortical development, we sought to approximate developmental variation in the effect of PRS-SCZ by esti-mating age group effects of early childhood (3–9 years), early adolescence (10–15 years), and late adolescence (16–21 years) in the cohort. Because of the smaller sample sizes within each age group, effects were in general smaller compared with the main effect and did not survive multiple comparison correc-tions, with the exception of a small cluster in the right rostral anterior cingulate cortex for the early childhood group. Higher PRS-SCZ was associated with greater cortical thickness in early childhood. However, the pattern differed in the older age groups (Figure 5). We detected a significant difference in the correlation coefficients between early childhood and late adolescence ($z = 2.84$, $p = .002$), as well as early adolescence and late adolescence ($z = 1.84$, $p = .033$). Furthermore, PRS-SCZ–related cortical thickness increases in early childhood correlated negatively with schizophrenia-related cortical ab-normalities, whereas PRS-SCZ–related cortical thinning in late adolescents correlated positively (Figure 5). To further inspect the age-related change in the PRS-SCZ effect on cortical thickness, we repeated the analysis using the entire cohort and iteratively shifting the age centering from 3 to 21 in 1-year in-tervals. Higher PRS-SCZ was associated with greater cortical thickness in the 3- to 6-year age-centered models (Figure S4), closely resembling the results from the main analysis (Figure 1C), and survived multiple comparison corrections (Figure S4 bottom) (RFT corrected, $p < .01$). Finally, the

observed nonlinear relation of PRS-SCZ on cortical thickness across different age groups was confirmed when examining the interaction effect of PRS-SCZ and Age^2 on cortical thick-ness across the entire age range 3–21 years (Figure S5).

DISCUSSION

Combining imaging genetics with multiscale mapping, we characterized the effect of PRS-SCZ on cortical morphometry across different scales of cortical organization. We found that higher PRS-SCZ was associated with greater cortical thick-ness in typically developing children and adolescents, while surface area and cortical volume showed only subtle associ-ations with PRS-SCZ. We further provided evidence that PRS-SCZ preferentially affects areas with heightened expression of dendrites and synapses and that the PRS-SCZ–related cortical differences accumulate in cytoarchitecturally and functionally defined cortical systems. We also found that the PRS-SCZ–related cortical pattern mirrors cortical thinning related to schizophrenia and other major psychiatric disorders. Finally, age group models suggested a potential trajectory from PRS-SCZ–associated cortical thickness increase in early childhood toward thinning in late adolescence, spatially resembling the adult brain phenotype of schizophrenia.

Our cell type–specific gene expression approach enabled cross-modal exploration of the relation of genetic risk for schizophrenia with expression levels of neurons and glia. Our findings support and extend upon postmortem analyses, which demonstrate abnormal dendritic and synaptic density in individuals with schizophrenia [see (74) for a recent meta-analysis]. Another recent study suggested that differences in cortical thickness across multiple psychiatric disorders (including schizophrenia) are associated with pyramidal cell gene expression, a gene set enriched for biological processes of dendrites (e.g., dendritic arborization and branching) (75), as well as synaptic function (32). The present findings extend this
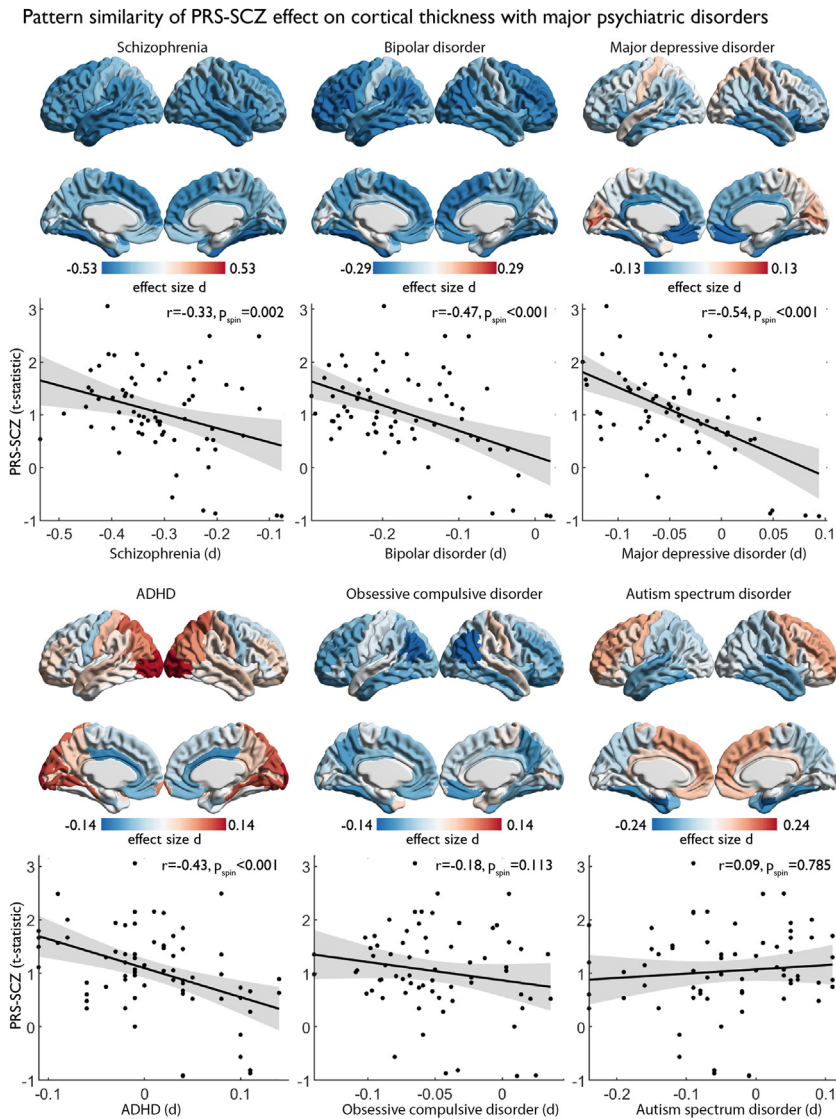
Figure 4. Pattern similarity of polygenic risk scores for schizophrenia (PRS-SCZ) on cortical thickness with major psychiatric disorders. Cortical surfaces show the effect size of schizophrenia, bipolar disorder, major depressive disorder, attention-deficit/hyperactivity disorder (ADHD), obsessive-compulsive disorder, and autism spectrum disorder diagnosis on cortical thickness from ENIGMA (Enhancing Neuro Imaging Genetics through Meta Analysis) meta-analyses of each disorder (63). Statistical significance was deemed where $p_{spin} < .025$ (two-tailed test) and false discovery rate (FDR) ($p_{FDR} < .05$) was applied to control for multiple comparisons ($n = 6$). Scatterplots show the correlation of each map with PRS-SCZ effect on cortical thickness.

work by demonstrating a relation between gene expression of dendrites and synapses with PRS-SCZ–related cortical differences during neurodevelopment.

System-specific contextualization revealed that PRS-SCZ effects on cortical thickness were spatially distributed, with the ventral attention network being preferentially sensitive to PRS-SCZ, while koniocortical type cortex was mostly spared from its influence. This cortical thickness pattern of PRS-SCZ closely mirrors recent observations in patients with schizophrenia showing stronger brain abnormalities in the ventral
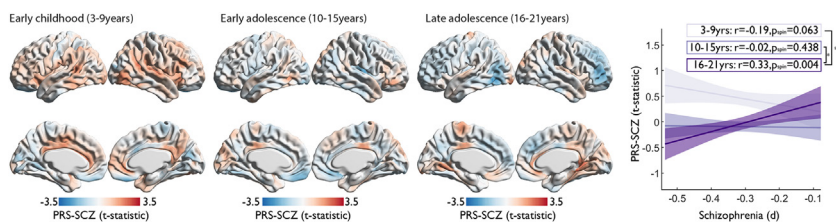

Figure 5. Age group–based polygenic risk scores for schizophrenia (PRS-SCZ) effect on cortical thickness. Cortical surfaces show unthresholded maps of PRS-SCZ effect on cortical thickness within age groups. Line plot shows how the relationship (linear regression with 95% confidence intervals) of PRS-SCZ with the SCZ-related pattern of abnormalities (Figure 4) changes from negative to positive across the age groups. Significant difference in correlation coefficients: $*p < .05$ and $**p < .01$.

attention network, while primary cortex, as defined by von Economo, was relatively spared (33). Altogether, these findings demonstrate that system-specific differentiations of PRS-SCZ–related cortical thickness differences during neurodevelopment reflect cortical abnormalities of schizophrenia, suggesting some neuroanatomical continuity between polygenic risk and clinical phenotype.

Longitudinal data and case-control meta-analysis have shown that the development of psychosis in high-risk adolescents is associated with progressive loss of cortical thickness in several areas of the association cortex (18,76). Of note, the areas implicated in these studies overlap considerably with those showing increased cortical thickness in early childhood and more pronounced cortical thinning in adolescents with higher PRS-SCZ in this study. We further observed that the pattern of PRS-SCZ–related cortical thickening was associated with areas of cortical thinning in schizophrenia, BD, MDD, and ADHD. This cross-disorder overlap notably mirrors the genetic and phenotypic correlation between these disorders (32,77) and is in line with recent work in neurodevelopmental cohorts reporting a transdiagnostic mode of genome-connectome covariation (78) and shared features of fronto-temporal dysconnectivity of general psychopathology (79). Collectively, these findings support the relevance of trans-diagnostic gene-brain and brain-psychopathology phenotypes during neurodevelopment. While we do not know the cause of increased cortical thickness in our sample, converging evidence supports the idea that reduced cortical thickness in adults with schizophrenia results from loss of neuropil, and specifically synapses. For example, postmortem studies in schizophrenia demonstrate synaptic loss (74); many genes implicated in schizophrenia are associated with synapses or synaptic pruning (5,80,81); and regional variations in cortical thickness correlate with neuropil (69). It is conceivable that the PRS-SCZ is associated with delayed pruning and an excess of synapses for age, which in turn may render the affected brain regions vulnerable to catastrophic synaptic loss during the emergence of psychosis.

The association of PRS-SCZ with greater cortical thickness in early childhood raises the question of how the genetic risk of schizophrenia contributes to abnormal developmental trajectories. Given that the transmodal areas identified in this analysis, such as the insula, exhibit modest cortical thinning from 3 to 21 years (82–84), our results align with an amplified trajectory (i.e., higher peak, steeper decline) and/or delayed cortical thinning in early childhood. Related to the complexity and heterochronicity of cortical maturation during childhood and adolescents (82), polygenic disorders can involve multiple types of abnormal trajectories, occurring simultaneously or sequentially (85,86). Amplified or delayed trajectory of trans-modal area morphometry may represent a core motif of cortical development in children with high PRS-SCZ. The PRS-SCZ includes multiple genetic factors, however, and their individual variation may produce heterogeneity in cortical development within high PRS-SCZ individuals.

The lack of associations between PRS-SCZ and surface area is in line with previous observations in adults (22) and meta-analytic evidence showing weaker surface area abnormalities compared to cortical thickness in schizophrenia (15). The divergent effects of PRS-SCZ on cortical thickness and

surface area observed in this study might further be explained by different underlying genetic architecture of both cortical features. The mechanisms underlying cortical thickness versus surface area are often placed in the context of Rakic's radial unit hypothesis, which proposes that surface area reflects the number of cortical columns, while thickness reflects the volume of each column (87). Using bioinformatic analyses, Grasby *et al.* (88) revealed that cortical thickness is influenced by genetic variants reflecting processes during mid fetal development including, myelination, branching, and pruning, while total surface area has been related to altered gene regulation in neural progenitor cells during fetal development. Collectively, these findings suggest that schizophrenia-related genetic variations exert a greater influence on neurodevelopmental processes altering cortical thickness than surface area.

This study should be interpreted in light of the cross-sectional nature of the dataset, which limits the ability to map individual longitudinal trajectories. The convergence of the observed findings with gene expression and neuroanatomical studies of schizophrenia support multiscale continuity between polygenic risk and clinical phenotype of schizophrenia. However, given the low familial risk and the relative absence of other biological or environmental risk factors for schizophrenia in the study cohort, interaction between PRS-SCZ and other biological and environmental risk factors could not directly be assessed and warrants further investigation. In addition, although mapping polygenic risk profiles on neuroimaging-derived phenotypes is a useful approach to further our understanding of genetic influence on neuroanatomical signatures related to schizophrenia risk, this method is limited by the fact that it does not allow direct translation into underlying biological mechanisms. Future research could therefore be enhanced by larger datasets with longitudinal designs and longer follow-up to determine which individuals will develop psychosis or other mental disorders. Finally, the observed PRS-SCZ–related cortical thickness increase in early childhood (age 3–9) highlights the need for large-scale initiatives targeting this age range.

Conclusions

This study provides novel evidence on the cellular basis and developmental trajectory of cortical thickness differences related to genetic risk for schizophrenia that may help to refine the neurodevelopmental hypothesis of schizophrenia. More generally, this work illustrates how maps of cortical organization can enrich descriptions of imaging-derived phenotypes related to genetic risk for mental illnesses. Altogether, this integrative framework combining imaging genetics and multi-scale mapping could advance our understanding of the complex associations between individual genetic profiles and cortical organization across multiple psychiatric and neurologic conditions.

ARTICLE INFORMATION

From the Montreal Neurological Institute, McGill University, Montreal, Québec, Canada (MK, CP, BSK, UV, NB, BH-S, NBA, BM, BCB, ACE, AD); Department of Psychiatry, Psychotherapy and Psychosomatics, Psychiatric Hospital, University of Zürich, Zürich, Switzerland (MK, FG); Division of Adult Psychiatry, Department of Psychiatry, University Hospitals of Geneva, Geneva, Switzerland (MK); Institute of Neuroscience and Medicine, Forschungszentrum Jülich, Jülich, Germany (CP); and Institute of Psychology, Faculty of Social Sciences, Tartu, Estonia (UV).

MK and CP contributed equally to this work.

Address correspondence to Matthias Kirschner, M.D., at matthiaskirschner@gmail.com, or Alain Dagher, M.D., at alain.dagher@mcgill.ca.

REFERENCES

1. Birnbaum R, Weinberger DR (2017): Genetic insights into the neurodevelopmental origins of schizophrenia. Nat Rev Neurosci 18:727–740.
2. Insel TR (2010): Rethinking schizophrenia. Nature 468:187–193.
3. Rapoport JL, Giedd JN, Gogtay N (2012): Neurodevelopmental model of schizophrenia: Update 2012. Mol Psychiatry 17:1228–1238.
4. Kessler RC, Angermeyer M, Anthony JC, DE Graaf R, Demyttenaere K, Gasquet I, et al. (2007): Lifetime prevalence and age-of-onset distributions of mental disorders in the World Health Organization's World Mental Health Survey Initiative. World Psychiatry 6:168–176.
5. Schizophrenia Working Group of the Psychiatric Genomics Consortium (2014): Biological insights from 108 schizophrenia-associated genetic loci. Nature 511:421–427.
6. Shaw P, Greenstein D, Lerch J, Clasen L, Lenroot R, Gogtay N, et al. (2006): Intellectual ability and cortical development in children and adolescents. Nature 440:676–679.
7. Raznahan A, Shaw P, Lalonde F, Stockman M, Wallace GL, Greenstein D, et al. (2011): How does your cortex grow? J Neurosci 31:7174–7177.
8. Khundrakpam BS, Lewis JD, Kostopoulos P, Carbonell F, Evans AC (2017): Cortical thickness abnormalities in autism spectrum disorders through late childhood, adolescence, and adulthood: A large-scale MRI study. Cereb Cortex 27:1721–1731.
9. Park BY, Bethlehem RA, Paquola C, Larivière S, Rodríguez-Cruces R, Vos de Wael R, et al. (2021): An expanding manifold in transmodal regions characterizes adolescent reconfiguration of structural connectome organization. Elife 10:e64694.
10. Sydnor VJ, Larsen B, Bassett DS, Alexander-Bloch A, Fair DA, Liston C, et al. (2021): Neurodevelopment of the association cortices: Patterns, mechanisms, and implications for psychopathology. Neuron 109:2820–2846.
11. Tamnes CK, Herting MM, Goddings AL, Meuwese R, Blakemore SJ, Dahl RE, et al. (2017): Development of the cerebral cortex across adolescence: A multisample study of inter-related longitudinal changes in cortical volume, surface area, and thickness. J Neurosci 37:3402–3412.
12. Giedd JN, Blumenthal J, Jeffries NO, Castellanos FX, Liu H, Zijdenbos A, et al. (1999): Brain development during childhood and adolescence: A longitudinal MRI study. Nat Neurosci 2:861–863.
13. Gogtay N, Giedd JN, Lusk L, Hayashi KM, Greenstein D, Vaituzis AC, et al. (2004): Dynamic mapping of human cortical development during childhood through early adulthood. Proc Natl Acad Sci U S A 101:8174–8179.
14. Paquola C, Bethlehem RA, Seidlitz J, Wagstyl K, Romero-Garcia R, Whitaker KJ, et al. (2019): Shifts in myeloarchitecture characterise adolescent development of cortical gradients. Elife 8:e50482.
15. van Erp TGM, Walton E, Hibar DP, Schmaal L, Jiang W, Glahn DC, et al. (2018): Cortical brain abnormalities in 4474 individuals with schizophrenia and 5098 control subjects via the Enhancing Neuro Imaging Genetics through Meta Analysis (ENIGMA) consortium. Biol Psychiatry 84:644–654.
16. Wannan CMJ, Cropley VL, Chakravarty MM, Bousman C, Ganella EP, Bruggemann JM, et al. (2019): Evidence for network-based cortical thickness reductions in schizophrenia. Am J Psychiatry 176:552–563.
17. Kirschner M, Shafiei G, Markello RD, Makowski C, Talpalaru A, Hodzic-Santor B, et al. (2020): Latent clinical-anatomical dimensions of schizophrenia. Schizophr Bull 46:1426–1438.
18. ENIGMA Clinical High Risk for Psychosis Working Group, Jalbrzikowski M, Hayes RA, Wood SJ, Nordholm D, Zhou JH, et al. (2021): Association of structural magnetic resonance imaging measures with psychosis onset in individuals at clinical high risk for developing psychosis: An ENIGMA working group mega-analysis. JAMA Psychiatry 78:753–766.
19. French L, Gray C, Leonard G, Perron M, Pike GB, Richer L, et al. (2015): Early cannabis use, polygenic risk score for schizophrenia, and brain maturation in adolescence. JAMA Psychiatry 72:1002–1011.
20. Liu B, Zhang X, Cui Y, Qin W, Tao Y, Li J, et al. (2017): Polygenic risk for schizophrenia influences cortical gyrification in 2 independent general populations. Schizophr Bull 43:673–680.
21. Neilson E, Bois C, Gibson J, Duff B, Watson A, Roberts N, et al. (2017): Effects of environmental risks and polygenic loading for schizophrenia on cortical thickness. Schizophr Res 184:128–136.
22. Neilson E, Shen X, Cox SR, Clarke TK, Wigmore EM, Gibson J, et al. (2019): Impact of polygenic risk for schizophrenia on cortical structure in UK Biobank. Biol Psychiatry 86:536–544.
23. Van der Auwera S, Wittfeld K, Homuth G, Teumer A, Hegenscheid K, Grabe HJ (2015): No association between polygenic risk for schizophrenia and brain volume in the general population. Biol Psychiatry 78:e41–e42.
24. Van der Auwera S, Wittfeld K, Shumskaya E, Bralten J, Zwiers MP, Onnink AM, et al. (2017): Predicting brain structure in population-based samples with biologically informed genetic scores for schizophrenia. Am J Med Genet B Neuropsychiatr Genet 174:324–332.
25. Reus LM, Shen X, Gibson J, Wigmore E, Ligthart L, Adams MJ, et al. (2017): Association of polygenic risk for major psychiatric illness with subcortical volumes and white matter integrity in UK Biobank. Sci Rep 7:42140.
26. Feinberg I (1982): Schizophrenia: Caused by a fault in programmed synaptic elimination during adolescence? J Psychiatr Res 17:319–334.
27. Sellgren CM, Gracias J, Watmuff B, Biag JD, Thanos JM, Whittredge PB, et al. (2019): Increased synapse elimination by microglia in schizophrenia patient-derived models of synaptic pruning. Nat Neurosci 22:374–385.
28. Sprooten E, O'Halloran R, Dinse J, Lee WH, Moser DA, Doucet GE, et al. (2019): Depth-dependent intracortical myelin organization in the living human brain determined by in vivo ultra-high field magnetic resonance imaging. Neuroimage 185:27–34.
29. Wei W, Zhang Y, Li Y, Meng Y, Li M, Wang Q, et al. (2020): Depth-dependent abnormal cortical myelination in first-episode treatment-naïve schizophrenia. Hum Brain Mapp 41:2782–2793.

30. Zhu Y, Sousa AMM, Gao T, Skarica M, Li M, Santpere G, et al. (2018): Spatiotemporal transcriptomic divergence across human and macaque brain development. Science 362:eaat8077.

31. Seidlitz J, Nadig A, Liu S, Bethlehem RAI, Vértes PE, Morgan SE, et al. (2020): Transcriptomic and cellular decoding of regional brain vulnerability to neurogenetic disorders [published correction appears in Nat Commun. 2020;11:5936]. Nat Commun 11:3358.

32. Writing Committee for the Attention-Deficit/Hyperactivity Disorder, Autism Spectrum Disorder, Bipolar Disorder (2021): Virtual histology of cortical thickness and shared neurobiology in 6 psychiatric disorders [published correction appears in JAMA Psychiatry. 2021;78:112]. JAMA Psychiatry 78:47–63.

33. Shafiei G, Markello RD, Makowski C, Talpalaru A, Kirschner M, Devenyi GA, et al. (2020): Spatial patterning of tissue volume loss in schizophrenia reflects brain network architecture. Biol Psychiatry 87:727–735.

34. Cao H, Zhou H, Cannon TD (2021): Functional connectome-wide associations of schizophrenia polygenic risk. Mol Psychiatry 26:2553–2561.

35. García-Cabezas MÁ., Hacker JL, Zikopoulos B (2020): A protocol for cortical type analysis of the human neocortex applied on histological samples, the atlas of von economo and Koskinas, and magnetic resonance imaging. Front Neuroanat 14:576015.

36. Yeo BT, Krienen FM, Sepulcre J, Sabuncu MR, Lashkari D, Hollinshead M, et al. (2011): The organization of the human cerebral cortex estimated by intrinsic functional connectivity. J Neurophysiol 106:1125–1165.

37. Jernigan TL, Brown TT, Hagler DJ Jr, Akshoomoff N, Bartsch H, Newman E, et al. (2016): The pediatric imaging, neurocognition, and genetics (PING) data repository. Neuroimage 124:1149–1154.

38. Khundrakpam B, Vainik U, Gong J, Al-Sharif N, Bhutani N, Kiar G, et al. (2020): Neural correlates of polygenic risk score for autism spectrum disorders in general population. Brain Commun 2:fcaa092.

39. Disorder Bipolar, Schizophrenia Working Group of the Psychiatric Genomics Consortium (2018): Genomic dissection of bipolar disorder and schizophrenia, including 28 subphenotypes. Cell 173:1705–1715.e16.

40. Choi SW, O'Reilly PF (2019): PRSice-2: Polygenic Risk Score software for biobank-scale data. GigaScience 8:giz082.

41. Ad-Dab'bagh Y, Einarson D, Lyttelton O, Muehlboeck J-S, Mok K, Ivanov O, et al. (2006). The CIVET Image-Processing Environment: A Fully Automated Comprehensive Pipeline for Anatomical Neuroimaging Research, vol. 1).

42. Worsley K, Taylor JP, Carbonell F, Chung M, Duerden EG, Bernhardt B, et al. (2009): SurfStat: A MATLAB toolbox for the statistical analysis of univariate and multivariate surface and volumetric data using linear mixed effects models and random field theory. Neuroimage 47:S102.

43. Hayasaka S, Phan KL, Liberzon I, Worsley KJ, Nichols TE (2004): Nonstationary cluster-size inference with random field and permutation methods. Neuroimage 22:676–687.

44. Worsley KJ, Taylor JE, Tomaiuolo F, Lerch J (2004): Unified univariate and multivariate random field theory. Neuroimage 23(Suppl 1):S189–S195.

45. Herculano-Houzel S, Watson CR, Paxinos G (2013): Distribution of neurons in functional areas of the mouse cerebral cortex reveals quantitatively different cortical zones. Front Neuroanat 7:35.

46. Li M, Santpere G, Imamura Kawasawa Y, Evgrafov OV, Gulden FO, Pochareddy S, et al. (2018): Integrative functional genomic analysis of human brain development and neuropsychiatric risks. Science 362:eaat7615.

47. Ashburner M, Ball CA, Blake JA, Botstein D, Butler H, Cherry JM, et al. (2000): Gene Ontology: Tool for the unification of biology. The Gene Ontology Consortium. Nat Genet 25:25–29.

48. The Gene Ontology Consortium (2019): The Gene Ontology Resource: 20 years and still GOing strong. Nucleic Acids Res 47:D330–D338.

49. Kang HJ, Kawasawa YI, Cheng F, Zhu Y, Xu X, Li M, et al. (2011): Spatio-temporal transcriptome of the human brain. Nature 478:483–489.

50. Paquola C, Seidlitz J, Benkarim O, Royer J, Klimes P, Bethlehem RAI, et al. (2020): A multi-scale cortical wiring space links cellular architecture and functional dynamics in the human brain. PLoS Biol 18:e3000979.

51. Park B, Kebets V, Larivière S, Hettwer MD, Paquola C, Rooij D, et al. (2022): Multilevel neural gradients reflect transdiagnostic effects of major psychiatric conditions on cortical morphology. Commun Biol 5:1024 (2022).

52. Paquola C, Garber M, Frässle S, Royer J, Tavakol S, Rodriguez-Cruces R, et al. (2021): The unique cytoarchitecture and wiring of the human default mode network. bioRxiv. https://doi.org/10.1101/2021.11.22.469533.

53. von Economo CF, Koskinas GN (1925): Die cytoarchitektonik der hirnrinde des erwachsenen menschen. J Springer.

54. Scholtens LH, de Reus MA, de Lange SC, Schmidt R, van den Heuvel MP (2018): An MRI Von Economo – Koskinas atlas. Neuroimage 170:249–256.

55. Alexander-Bloch AF, Shou H, Liu S, Satterthwaite TD, Glahn DC, Shinohara RT, et al. (2018): On testing for spatial correspondence between maps of human brain structure and function. Neuroimage 178:540–551.

56. Burt JB, Helmer M, Shinn M, Anticevic A, Murray JD (2020): Generative modeling of brain maps with spatial autocorrelation. Neuroimage 220:117038.

57. Desikan RS, Ségonne F, Fischl B, Quinn BT, Dickerson BC, Blacker D, et al. (2006): An automated labeling system for subdividing the human cerebral cortex on MRI scans into gyral based regions of interest. Neuroimage 31:968–980.

58. Schmaal L, Hibar DP, Sämann PG, Hall GB, Baune BT, Jahanshad N, et al. (2017): Cortical abnormalities in adults and adolescents with major depression based on brain scans from 20 cohorts worldwide in the ENIGMA Major Depressive Disorder Working Group. Mol Psychiatry 22:900–909.

59. Hibar DP, Westlye LT, Doan NT, Jahanshad N, Cheung JW, Ching CRK, et al. (2018): Cortical abnormalities in bipolar disorder: An MRI analysis of 6503 individuals from the ENIGMA Bipolar Disorder Working Group. Mol Psychiatry 23:932–942.

60. Hoogman M, Muetzel R, Guimaraes JP, Shumskaya E, Mennes M, Zwiers MP, et al. (2019): Brain imaging of the cortex in ADHD: A coordinated analysis of large-scale clinical and population-based samples. Am J Psychiatry 176:531–542.

61. Boedhoe PSW, Schmaal L, Abe Y, Alonso P, Ameis SH, Anticevic A, et al. (2018): Cortical abnormalities associated with pediatric and adult obsessive–compulsive disorder: Findings from the ENIGMA obsessive–compulsive disorder working group. Am J Psychiatry 175:453–462.

62. van Rooij D, Anagnostou E, Arango C, Auzias G, Behrmann M, Busatto GF, et al. (2018): Cortical and subcortical brain morphometry differences between patients with autism spectrum disorder and healthy individuals across the lifespan: Results from the ENIGMA ASD working group. Am J Psychiatry 175:359–369.

63. Larivière S, Paquola C, Park BY, Royer J, Wang Y, Benkarim O, et al. (2021): The ENIGMA Toolbox: Multiscale neural contextualization of multisite neuroimaging datasets. Nat Methods 18:698–700.

64. Markello RD, Misic B (2021): Comparing spatial null models for brain maps. Neuroimage 236:118052.

65. Sawyer SM, Azzopardi PS, Wickremarathne D, Patton GC (2018): The age of adolescence. Lancet Child Adolesc Health 2:223–228.

66. Meng X, Rosenthal R, Rubin DB (1992): Comparing correlated correlation coefficients. Psychol Bull 111:172–175.

67. Collins CE, Airey DC, Young NA, Leitch DB, Kaas JH (2010): Neuron densities vary across and within cortical areas in primates. Proc Natl Acad Sci U S A 107:15927–15932.

68. Cahalane DJ, Charvet CJ, Finlay BL (2012): Systematic, balancing gradients in neuron density and number across the primate isocortex. Front Neuroanat 6:28.

69. Carlo CN, Stevens CF (2013): Structural uniformity of neocortex, revisited. Proc Natl Acad Sci U S A 110:1488–1493.

70. Braitenberg V, Schüz A (1998): Density of axons. In: Braitenberg V, Schüz A, editors. Cortex: Statistics and geometry

of neuronal connectivity. Berlin, Heidelberg: Springer Berlin Heidelberg, 39–42.

71. von EC (2009): Cellular structure of the human cerebral cortex. In: Triarhou LC, editor. Plus poster: 'The 107 Cortical Cytoarchitectonic Areas of Constantin von Economo and Georg N. Koskinas in the Adult Human Brain.' Available at: https://www.karger.com/Book/Home/247637. Bâle: Karger. Accessed January 16, 2021.

72. Diedenhofen B, Musch J (2015): cocor: A Comprehensive Solution for the Statistical Comparison of Correlations [published correction appears in PLoS One. 2015;10:e0131499]. PLoS One 10:e0121945.

73. Zou GY (2007): Toward using confidence intervals to compare correlations. Psychol Methods 12:399–413.

74. Berdenis van Berlekom A, Muflihah CH, Snijders GJLJ, MacGillavry HD, Middeldorp J, Hol EM, et al. (2020): Synapse pathology in schizophrenia: A meta-analysis of postsynaptic elements in postmortem brain studies. Schizophr Bull 46:374–386.

75. Srinivas KV, Buss EW, Sun Q, Santoro B, Takahashi H, Nicholson DA, Siegelbaum SA (2017): The dendrites of CA2 and CA1 pyramidal neurons differentially regulate information flow in the cortico-hippocampal circuit. J Neurosci 37:3276–3293.

76. Cannon TD, Chung Y, He G, Sun D, Jacobson A, van Erp TG, et al. (2015): Progressive reduction in cortical thickness as psychosis develops: A multisite longitudinal neuroimaging study of youth at elevated clinical risk. Biol Psychiatry 77:147–157.

77. Brainstorm Consortium, Anttila V, Bulik-Sullivan B, Finucane HK, Walters RK, Bras J, et al. (2018): Analysis of shared heritability in common disorders of the brain. Science 360:eaap8757.

78. Taquet M, Smith SM, Prohl AK, Peters JM, Warfield SK, Scherrer B, Harrison PJ (2021): A structural brain network of genetic vulnerability to psychiatric illness. Mol Psychiatry 26:2089–2100.

79. Alnæs D, Kaufmann T, van der Meer D, Córdova-Palomera A, Rokicki J, Moberget T, et al. (2019): Brain heterogeneity in schizophrenia and its association with polygenic risk [published correction appears in JAMA Psychiatry. 2019]. JAMA Psychiatry 76:739–748.

80. Kirov G, Pocklington AJ, Holmans P, Ivanov D, Ikeda M, Ruderfer D, et al. (2012): De novo CNV analysis implicates specific abnormalities of postsynaptic signalling complexes in the pathogenesis of schizophrenia. Mol Psychiatry 17:142–153.

81. The Schizophrenia Working Group of the Psychiatric Genomics Consortium, Ripke S, Walters JTR, O'Donovan MC (2020): Mapping genomic loci prioritises genes and implicates synaptic biology in schizophrenia. medRxiv. https://doi.org/10.1101/2020.09.12.20192922.

82. Ball G, Beare R, Seal ML (2019): Charting shared developmental trajectories of cortical thickness and structural connectivity in childhood and adolescence. Hum Brain Mapp 40:4630–4644.

83. Sotiras A, Toledo JB, Gur RE, Gur RC, Satterthwaite TD, Davatzikos C (2017): Patterns of coordinated cortical remodeling during adolescence and their associations with functional specialization and evolutionary expansion. Proc Natl Acad Sci U S A 114:3527–3532.

84. Zielinski BA, Prigge MBD, Nielsen JA, Froehlich AL, Abildskov TJ, Anderson JS, et al. (2014): Longitudinal changes in cortical thickness in autism and typical development. Brain 137:1799–1812.

85. Di Martino A, Fair DA, Kelly C, Satterthwaite TD, Castellanos FX, Thomason ME, et al. (2014): Unraveling the miswired connectome: A developmental perspective. Neuron 83:1335–1353.

86. Klingler E, Francis F, Jabaudon D, Cappello S (2021): Mapping the molecular and cellular complexity of cortical malformations. Science 371:eaba4517.

87. Rakic P, Ayoub AE, Breunig JJ, Dominguez MH (2009): Decision by division: Making cortical maps. Trends Neurosci 32:291–301.

88. Grasby KL, Jahanshad N, Painter JN, Colodro-Conde L, Bralten J, Hibar DP, et al. (2020): The genetic architecture of the human cerebral cortex [published correction appears in Science. 2021;374:eabm7211]. Science 367:eaay6690.